Communication

Ligand-Directed Dynamics of Adenine Riboswitch Conformers

Saman Eskandari, Oksana Prychyna, Jessica Leung, Dijana Avdic, and Melanie A. O'Neill

J. Am. Chem. Soc., **2007**, 129 (37), 11308-11309• DOI: 10.1021/ja073159l • Publication Date (Web): 22 August 2007

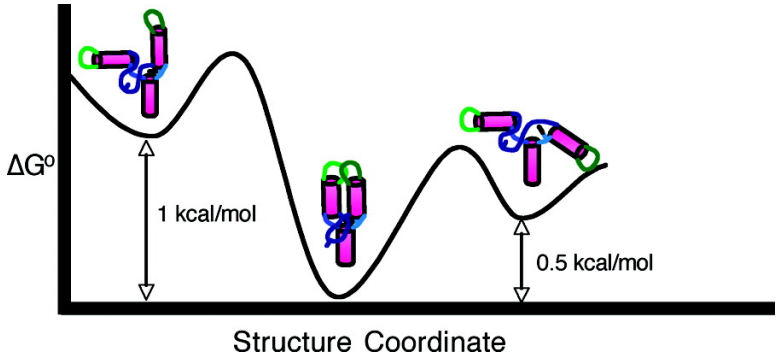

More About This Article

Additional resources and features associated with this article are available within the HTML version:

- Supporting Information
- Access to high resolution figures
- Links to articles and content related to this article
- Copyright permission to reproduce figures and/or text from this article

View the Full Text HTML

J|A|C|S
COMMUNICATIONS

Published on Web 08/22/2007

Ligand-Directed Dynamics of Adenine Riboswitch Conformers

Saman Eskandari, Oksana Prychyna, Jessica Leung, Dijana Avdic, and Melanie A. O'Neill*

Department of Chemistry, Simon Fraser University, Burnaby, British Columbia, Canada, V5A 1S6

Received May 4, 2007; E-mail: maoneill@sfu.ca

Riboswitches are conserved, non-coding mRNAs that regulate gene expression in response to specific ligand binding.[1] Structural[2−6] and mechanistic studies[3,7−10] aimed at understanding RNA−ligand interactions have focused on purine riboswitches: Despite virtually identical secondary and tertiary structures, these riboswitches exhibit ~10^5-fold discrimination between G and A.[9] The ligand binding (aptamer) domain of these riboswitches (GRNA, ARNA, Figure 1) consists of three paired stems joined by a conserved three-way junction that forms the binding site; P1 is linked to the expression platform, while the ends of P2 and P3 are capped by conserved loops (L2, L3). Swapping a single nucleotide, N65 (ARNA numbering) U/C, exchanges the A/G specificity of riboswitch binding in vitro.[9] This has been attributed to Watson−Crick pairing, seen in high-resolution structures where the N65−ligand pair is buried by junction and L2−L3 interactions that close the binding site and P2−P3 stems. These static structures do not reveal how RNA dynamics couple to recognition. We show here that *ligand-bound* ARNA adopts multiple, globally distinct conformers in solution. Ligand-directed conformer dynamics are proposed to be key to riboswitch recognition and gene regulation.

Slow, biphasic ligand binding kinetics[3,10] have prompted induced fit models where conformationally heterogeneous free RNA folds to a single highly ordered RNA−ligand structure. In free RNA, P1, P2, and P3 appear to be organized, while the junction and loops are conformationally dynamic.[3,6−9] Junction dynamics may modulate RNA structure locally at the binding pocket (e.g., N39 intra- or extrahelical);[3] this movement likely contributes to specific recognition by N65.[7] Junction dynamics may also couple to loop motion to modulate RNA structure globally (e.g., P2−P3 open, intermediate, or closed) as detected in single ARNA molecules.[8] These latter results are provocative as they contrast NMR findings that GRNA exhibits local junction dynamics but within a static global conformer (P2−P3 closed).[6] They also find similar dynamics in free and *bound* ARNA which contrasts with induced fit models and ensemble NMR evidence of a single bound structure for both ARNA and GRNA.[4−6] Given ~90% conservation of junction and loop residues in A and GRNA, why is ARNA more dynamic, especially when bound, and what are the functional consequences?

To address these central questions, we first sought to detect and characterize bound ARNA conformers in ensemble solution using time-resolved fluorescence spectroscopy. Interaction of the fluorescent adenine analogue, 2-aminopurine (Ap), with ARNA mimics that of A structurally, thermodynamically, and kinetically.[3,7−10] Since the fluorescence lifetime (τ) of Ap depends sensitively on the structure of DNA or RNA to which it is bound,[11] each Ap-ARNA conformer will have a unique τ. In an ensemble, conformers whose dynamic exchange is slow relative to this lifetime (i.e., > ~10 ns) will be resolved as components in a multiexponential fluorescence lifetime.

The fluorescence decay profile (Figure 2a)[12] of Ap-ARNA[13] differs dramatically from free Ap (τ = 11.5 ns, χ^2 ~ 1.2). The time-integrated emission yields the same ensemble-averaged

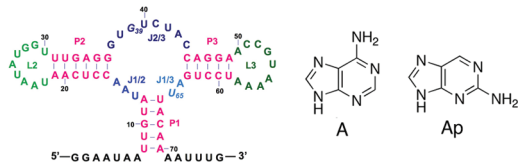

Figure 1. Secondary structure of the aptamer domain of the A riboswitch (pbuE, *Bacillus subtilis*) and molecular structure of two ligands, A and Ap.

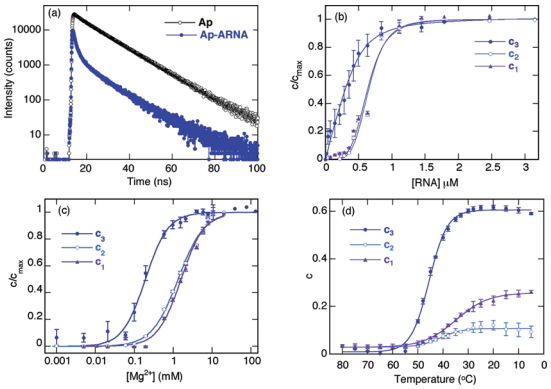

Figure 2. Characterization of Ap-ARNA with time-resolved fluorescence. (a) fluorescence decay of Ap and Ap-ARNA (500 nM Ap, 3.5 μM ARNA, 20 °C, 10 mM Mg^{2+}). Variation in amplitude (c) of static quenching (c_3), and lifetimes (c_2, c_1) of Ap-ARNA as a function of RNA concentration (b), Mg^{2+} concentration (c), and temperature (d).

dissociation constant for Ap-ARNA as steady-state measurements, K_D = 100 ± 50 nM (20 °C, 10 mM Mg^{2+}). However, the lifetime is not fit by either a single ($\chi^2 \geq 10$) or a double exponential decay ($\chi^2 \geq 3.5$), but is well modeled ($\chi^2 \leq 1.2$) by three exponentials.[14] We also observe static quenching, a reduction in the initial fluorescence intensity corresponding to an additional lifetime(s) beyond our instrument resolution.[15] Overall, our time-resolved fluorescence is described by $I(t) = c_u\tau_u + c_1\tau_1 + c_2\tau_2 + c_3\tau_3$ (Table 1). The longest lifetime (τ_u) matches free Ap, and we assign it to the unbound fraction (c_u).[16] We assign the two resolved lifetimes, τ_1 and τ_2, and the unresolved lifetime, τ_3,[17] to three different conformers C_1, C_2, and C_3, respectively, of Ap-ARNA.

Dissociation constants derived from steady-state fluorescence reflect binding affinities averaged over an ensemble of conformers. Here using variations in amplitude of each fluorescence lifetime component (c_n) we monitor binding in each Ap-ARNA conformer and find that they differ markedly for binding both Ap (Figure 2b) and Mg^{2+} (Figure 2c). This is evident visually as C_1 and C_2 show sigmoidal rather than hyperbolic responses to Ap and quantitatively in the K_D values (Table 1). Similarly, the Mg^{2+} binding affinity is an order of magnitude higher for C_3 than the other conformers, and C_2 binds Mg^{2+} ~1.5-fold more tightly than C_1. These binding affinities bracket ensemble-averaged values for Mg^{2+} binding to the A[8] or thiamine pyrophosphate riboswitches.[18]

Temperature does not significantly alter the fluorescence lifetimes of Ap-ARNA,[19] but it modulates the relative amplitudes of the

10.1021/ja073159l CCC: $37.00

Table 1. Characteristics of Ap-ARNA Conformers[a]

	C_1	C_2	C_3
τ (ns)[b]	1.9 ± 0.1[c]	0.5 ± 0.2[c]	<0.3[d]
c[b]	0.20 ± 0.05[c]	0.10 ± 0.05[c]	0.60 ± 0.05[d]
K_D Ap (nM)[e]	635 ± 25	653 ± 25	60 ± 50
K_D Mg (μM)[e]	2000 ± 100	1500 ± 100	90 ± 20
T_m (°C)	35 ± 1	41 ± 1	46 ± 1

[a] Averages of 3−6 experiments. [b] At 20 °C, 10 mM Mg^{2+}. [c] Fluorescence decay fit to $I(t) = c_u\tau_u + c_1\tau_1 + c_2\tau_2$; $c_u = 0.1$. [d] Value of τ less than time resolution; c_3 from statically quenched fraction. [e] Fit to hyperbolic or sigmoidal models (see Supporting Information).

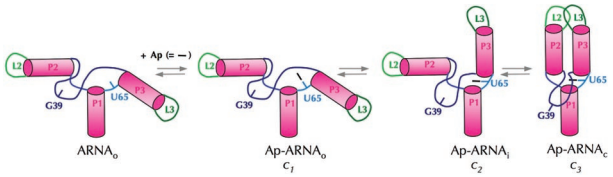

Figure 3. Ap binds an open conformer of free ARNA, generating at least three Ap-ARNA conformers schematized here. Through different arrangement of junction (blue), stems (pink), and loops (green), the conformers have distinct local (binding site) and global structures.

lifetime components (Figure 2d). From these, we derive melting temperatures (T_m) of 35, 41, and 46 °C for C_1, C_2 and C_3, respectively (Table 1). The thermal stability of the conformers parallels their binding affinity for Ap and Mg^{2+} with $C_3 > C_2 > C_1$.

The distinct fluorescence lifetimes, ligand binding affinities, and thermal stabilities of C_1, C_2, and C_3 characterize each as a unique Ap-ARNA conformer. Ap has the shortest lifetime in C_3; this conformer has the smallest K_D for Ap and Mg^{2+} and the highest thermal stability. These consistent results suggest that Ap is tightly bound in a tertiary structure compact relative to C_2 and C_1. This is reminiscent of purine riboswitch structures[2−6] where ligand is captured in an RNA conformation that is "closed" both locally at the binding pocket via junction interactions with N39 extrahelical and globally via L2−L3 hydrogen bonding that tightly aligns P2−P3. Given that this structure is seen in solid state and solution bound to several purines,[2−6] we fully expect it in our ensemble and assign C_3 to this closed conformer, Ap-ARNA$_c$ (Figure 3).

The weaker binding affinity and longer fluorescence lifetimes of Ap indicate that it is poorly stacked in C_2 and C_1; clearly distinct from C_3, these conformers are likely "open" at the binding pocket. The reduced Mg^{2+} binding affinity and T_m indicate that C_2 and C_1 have fewer tertiary contacts and less compact structures than C_3. Together these suggest that C_2 and C_1 *do not resemble* the purine riboswitch structures seen by crystallography or NMR, and, consistent with single molecule studies,[8] conformational dynamics persist in bound ARNA with the exchange being ligand-directed. Although we lack high-resolution information on C_2 and C_1, we can propose tractable models (Figure 3) for their structures from data reported here and previously.[3,7,8] We suggest that in C_1 the binding pocket and P2−P3 are open (Ap-ARNA$_o$). In C_3, L2−L3 interactions close P2−P3 and the binding pocket (Ap-RNA$_c$), while C_2 is an intermediate conformer where Ap is more stacked, but P2−P3 and the binding pocket are partially open (Ap-ARNA$_i$).[20]

That the global structures of C_2 and C_1 are distinct from C_3 is supported by their lower T_m and Mg^{2+} binding affinities. That C_2 and C_1 are P2−P3 open conformers is supported by mutagenesis where abrogating L2−L3 interactions substantially (>10-fold) lowers ligand binding affinity[8] as observed here. This model is further supported by single molecule detection of three discrete P2−P3 distances (open, intermediate, and closed) in *bound* ARNA.[8] In fact, rate constants for closing and opening of 1.5 and 0.84 s^{-1}, respectively,[8] yield an equilibrium constant of 1.8 and a free energy separation of only 0.3 kcal mol^{-1} between the closed and open/intermediate forms. We find the same values ($K_{eq} = 2$, $\Delta G = 0.4$ kcal mol^{-1}) from our conformer distribution (66% closed, 33% open/intermediate). Given that earlier experiments probed FRET from single, labeled RNAs,[8] while we probe ligand fluorescence in ensemble solution, the similarities are striking.

The emerging model for ARNA suggests that junction dynamics generate locally[3,7] and globally[8] distinct conformers in contrast with GRNA where dynamics do not alter global structure.[6] This is fascinating given their structural homology. These differences in dynamics may be at the root of the divergent specificity and function of G and A riboswitches. For ARNA, ligand-directed RNA dynamics yields multiple, energetically similar yet globally distinct ligand−RNA conformers.[21] These conformers are not high-energy, transient intermediates along the RNA folding pathway, but *together* represent the ensemble population. We hypothesize that only one bound ARNA conformer will be functionally active in gene regulation, and we are now testing factors that influence conformer distribution and its impact on riboswitch response. We predict that the balance of ligand binding kinetics and ligand-directed RNA folding will tune the conformer distribution and the potency of a ligand in riboswitch-mediated gene regulation.

Acknowledgment. We are grateful for support from Simon Fraser University, NSERC, and MSFHR. We thank Profs. Peter Unrau (Hani Zaher) and Dipankar Sen for their expertise and resources which significantly advanced our RNA program.

Supporting Information Available: Experimental methods, TC-SPC data and fits, description of K_D evaluation. This material is available free of charge via the Internet at http://pubs.acs.org.

References

(1) Winkler, W. C.; Breaker, R. R. *Annu. Rev. Microbiol.* **2005**, *59*, 487−517.
(2) Batey, R. T.; Gilbert, S. D.; Motange, R. K. *Nature* **2004**, *432*, 411−415.
(3) Gilbert, S. D.; Stoddard, C. D.; Wise, S. J.; Batey, R. T. *J. Mol. Biol.* **2006**, *359*, 754−768.
(4) Serganov, A.; Yuan, Y. R.; Pikovskaya, O.; Polonskaia, A.; Malinina, L.; Phan, A. T.; Hobartner, C.; Micura. R.; Breaker, R. R.; Patel, D. *J. Chem. Biol.* **2004**, *11*, 1729−1741.
(5) Noeske, J.; Richter, C.; Grundl, M. A.; Nasiri, H. R.; Schwalbe, H.; Wohnert, J. *Proc. Natl. Acad. Sci. U.S.A.* **2005**, *102*, 1372−1377.
(6) Noeske, J.; Buck, J.; Furtig, B.; Nasiri, H. R.; Schwalbe, H.; Wohnert, J. *Nucleic Acids Res.* **2007**, *35*, 572−583.
(7) Lemay, J. F.; Penedo, J. C.; Tremblay, R.; Lilley, D. M.; Lafontaine, D. A. *RNA* **2007**, *13*, 339−350.
(8) Lemay, J. F.; Penedo, J. C.; Tremblay, R.; Lilley, D. M.; Lafontaine, D. A. *Chem. Biol.* **2006**, *13*, 857−868.
(9) (a) Mandal, M.; Boese, B.; Barrick, J. E.; Winkler, W. C.; Breaker R. R. *Cell* **2003**, *113*, 577−586. (b) Mandal, M.; Breaker, R. R. *Nat. Struct. Mol. Biol.* **2004**, *11*, 29−35.
(10) Wickiser, J. K.; Cheah, M. T.; Breaker, R. R.; Crothers, D. M. *Biochemistry* **2005**, *44*, 13404−13414.
(11) Rist, M. J.; Marino, J. P. *Curr. Org. Chem.* **2002**, *6*, 775−793.
(12) From time-correlated single photon counting (Supporting Information).
(13) ARNA generated by in vitro transcription (Supporting Information).
(14) Inclusion of a fourth component did not significantly improve fits.
(15) We measure $\tau \geq 300$ ps. In nucleic acid duplexes, Ap has τ as low as ~10 ps.
(16) At 20 °C, 500 nM Ap, 3.5 μM RNA, 10 mM Mg^{2+}, we have ≥90% bound.
(17) We do not expect a complex distribution for the static component. We are currently using femtosecond fluorescence to resolve this component.
(18) Yamauchi, T.; Miyoshi, D.; Kubodera, T.; Nishimura, A.; Nakai, S.; Sugimoto, N. *FEBS Lett.* **2005**, *579*, 2583−2588.
(19) The fluorescence of Ap is temperature-dependent. The influence of temperature on Ap-ARNA is obtained by referencing to free Ap.
(20) We are currently testing our conformer assignment with mutagenesis.
(21) Favorable enthalpy of C_3 formation may be offset by entropic barriers to order RNA tertiary structure, Mg^{2+}, and water.

JA073159L